Experimental demonstration of tripartite entanglement versus tripartite nonlocality in three-qubit Greenberger-Horne-Zeilinger–class states

Huai-Xin Lu, Jia-Qiang Zhao, Xiao-Qin Wang, and Lian-Zhen Cao

Phys. Rev. A **84**, 012111 — Published 20 July 2011

DOI: 10.1103/PhysRevA.84.012111

Experimental Demonstration of Tripartite Entanglement versus Tripartite Nonlocality in Three-Qubit Greenberger-Horne-Zeilinger-Class States

Huai-Xin Lu,[1] Jia-Qiang Zhao,[1] Xiao-Qin Wang,[1] and Lian-Zhen Cao[1]

[1] *Department of Physics and Electronic Science, Weifang University, Weifang, Shandong 261061, China*

As stated by S. Ghose et al. [Phys. Rev. Lett. 102, 250404 (2009)], there are certain relationships between tripartite entanglement and tripartite nonlocality for three-qubit Greenberger-Horne-Zeilinger (GHZ) class states. In the present work, we have experimentally demonstrated the theoretical results in [Phys. Rev. Lett. 102, 250404 (2009)] by using both three-photon generalized GHZ (GGHZ) states and maximal slice (MS) states with a count of $\sim 10/s$. From the data, we have verified the agreement of the experimental violation of Svetlichny inequality with the one predicted by quantum mechanics given the reconstructed density matrix. For the MS states, it is demonstrated that the amount of violation increases linearly following the increase of the degree of tripartite entanglement. In contrast, for GGHZ states, there is a minimal value of the violation when the degree of tripartite entanglement is 1/3. Both of the results are consist with the theoretical prediction.

PACS numbers: 03.65.Ud, 42.65.Lm, 03.67.Bg, 03.67.Mn

Introduction — Quantum entanglement plays a crucial role in quantum information processing and the fundamental demonstration of quantum mechanics. Entangled states can be used to demonstrate the contradiction between local reality (LR) and quantum mechanics(QM) [1–4]. It is well known that pure entangled states of two qubits violate the Bell-type Clauser-Horner-Shimony-Holt (CHSH) inequality [5, 6], and the amount of violate increases with the degree of the bipartite entanglement [7, 8] in the state. The relationship between tripartite entanglement and genuine tripartite nonlocality for threequbit pure states in the Greenberger-Horne-Zeilinger class has been analyzed by S. Ghose et al. [9]. It is shown that there is unique relationship between tripartite entanglement versus tripartite nonlocality for different types of three-qubit entangled states, such as the generalized Greenberger-Horne-Zeilinger (GGHZ) states and maximal slice (MS) states. The investigation of Bell inequalities for three-qubit states has important meanings for both the practical applications and theoretical studies of quantum entangled states. They are found to have promising applications in the field of quantum communication such as dense coding [10], quantum teleportation [11]and quantum cryptography [12]. In addition, they are useful tools to investigate the entanglement properties of different types of entangled states and prove the genuine multi-party entanglement in the quantum states. Here we focus on the Svetlichny inequality, because its violation is a sufficient condition for the confirmation of genuine three-qubit nonlocal correlations [9].

In this paper, experimental demonstration of Svetlichny inequality with three-qubit GHZ states has been reported [13]. In this letter, we have demonstrated the test of Svetlichny the whole set of three-photon GGHZ states and MS states for the first time. With the method of quantum state tomography, we have reconstructed the detailed density matrices of the states and achieved the fidelities of the sources. The average of the fidelity is 0.84 ± 0.01 being comparable to the value in the recent work [13], while our intensity is $\sim 10/s$. With these sources, we report the experimental testing of Svetlichny inequality for three-qubit GGHZ states and MS states. Furthermore, we verified the unique relationship of tripartite entanglement versus tripartite nonlocality for each type of these quantum states, as predicted in Ref. [9].

Theory — Svetlichny considered a hybrid model of nonlocal-local realism where two of the qubits are nonlocally correlated, but are locally correlated to the third. The Svetlichny inequality is defined in terms of the expectation value of a Bell-type operator S, which is defined as

$$S = A(BK + B^{'}K^{'}) + A^{'}(BK^{'} - B^{'}K) \tag{1}$$

where $K = C + C^{'}$ and $K^{'} = C - C^{'}$. There are three spatially separated qubits, and the operator $A = \vec{a}\cdot\vec{\sigma_1}$ or $A^{'} = \vec{a^{'}}\cdot\vec{\sigma_1}$ are performed on qubit 1, $B = \vec{b}\cdot\vec{\sigma_2}$ or $B^{'} = \vec{b^{'}}\cdot\vec{\sigma_2}$ on qubit 2, $C = \vec{c}\cdot\vec{\sigma_3}$ or $C^{'} = \vec{c^{'}}\cdot\vec{\sigma_3}$ on qubit 3, where $\vec{a}$, $\vec{a^{'}}$, $\vec{b}$, $\vec{b^{'}}$ and $\vec{c}$, $\vec{c^{'}}$ are unit vectors, $\vec{\sigma_i}$ are spin projection operators and $\vec{a^{'}} = (sin\theta_a cos\phi_a, sin\theta_a sin\phi_a, cos\theta_a)$. If a theory is consistent with a hybrid model of nonlocal-local realism, the expectation value for any three-qubit state is bounded by Svetlichny inequality, $|\langle\psi|S|\psi\rangle| = S(\psi) \leq 4$.

The GGHZ state $\left|\psi_g\right\rangle$ and the MS states $|\psi_s\rangle$ are defined as follows [9]

$$\left|\psi_g\right\rangle = cos\theta_1\,|000\rangle + sin\theta_1\,|111\rangle, \tag{2}$$

$$|\psi_s\rangle = \frac{1}{\sqrt{2}}\{|000\rangle + |11\rangle\,(cos\theta_3\,|0\rangle + sin\theta_3\,|1\rangle)\}. \tag{3}$$

The maximum expectation value of S for the GGHZ and MS states is respectively

$$S_{max}(\psi_g) = \begin{cases} 4\sqrt{1-\tau(\psi_g)}, & \tau(\psi_g) \leq 1/3 \\ 4\sqrt{2\tau(\psi_g)}, & \tau(\psi_g) \geq 1/3 \end{cases} \tag{4}$$

$$S_{max}(\psi_s) = 4\sqrt{1+\tau(\psi_s)}, \tag{5}$$

where the three-tangle $\tau(\psi)$ quantifies tripartite entanglement [14], with $\tau(\psi_g) = sin^2 2\theta_1$ and $\tau(\psi_s) = sin^2\theta_3$. S. Ghose et al. show theoretically that, for MS states, the amount of violation increases linearly following the increase of the degree of tripartite entanglement; while for GGHZ states, $S_{max}(\psi_g)$ initially decreases monotonically with τ, and then increases for $\tau(\psi_g) > 1/3$.

According to the Ref. [9], to achieve $S_{max}(\psi_g)$ in Eq. (4), we could measure by the following possible sets of unit vectors: for $\tau(\psi_g) \leq 1/3$, $\vec{a}$, $\vec{a'}$, $\vec{b}$, $\vec{b'}$ and $\vec{c}$ are all aligned along $\vec{z}$, and $\vec{c'}$ is aligned along $-\vec{z}$; for $\tau(\psi_g) \geq 1/3$ all the measurement vectors lie in the $x-y$ plane with $\phi_{adc} = \phi_{ad'c'} = \phi_{a'd'c} = 0$, $\phi_{a'dc'} = \pi$, and $\phi_d - \phi_{d'} = \pi/2$, where ϕ_{ijk} is defined as $\phi_{ijk} = \phi_i + \phi_j + \phi_k$. The theoretical values of the lower and upper bounds are consist with the the numerical bounds in Ref. [15].

With respect to the MS state, a set of measurement angles which realize $S_{max}(\psi_s)$ in Eq. (5) is $\theta_a = \theta_{a'} = \theta_d = \theta_{d'} = \pi/2$. $tan\theta_c = tan\theta_{c'} = \sqrt{2}tan\theta_3$, $\phi_{adc} = \phi_{ad'c'} = \phi_{a'd'c} = 0$, $\phi_{ad'c'} = \pi$, $\phi_c = -\phi_{c'} = \pi/4$, $\phi_d - \phi_{d'} = \pi/2$. The only difference between these angles and the optimal measurement angles for the GGHZ states in the regime $\tau(\psi_g) > 1/3$ is that $\vec{c}$ and $\vec{c'}$ do not lie in the $x-y$ plane. In our experiment, we choose a set of special angles as table I.

	θ_a	$\theta_{a'}$	θ_c	$\theta_{c'}$	θ_d	$\theta_{d'}$
$\tau(\psi_g) \leq 1/3$	0	0	0	0	π	0
$\tau(\psi_g) \geq 1/3$	$\pi/2$	$\pi/2$	$\pi/2$	$\pi/2$	$\pi/2$	$\pi/2$
MS states	$\pi/2$	$\pi/2$	$arctan(\sqrt{2}tan\theta_3)$	$arctan(\sqrt{2}tan\theta_3)$	$\pi/2$	$\pi/2$
	ϕ_a	$\phi_{a'}$	ϕ_c	$\phi_{c'}$	ϕ_d	$\phi_{d'}$
$\tau(\psi_g) \leq 1/3$	/	/	/	/	/	/
$\tau(\psi_g) \geq 1/3$	$-\pi/2$	0	0	$\pi/2$	$\pi/2$	0
MS states	$\pi/4$	$-\pi/4$	$\pi/4$	$-\pi/4$	$\pi/2$	0

TABLE I: Special angles chosen in our experiment. Several special angle $\theta_3 = 90°, 58°, 40°$, and $22°$, can be derived from the experiment data. From θ_3, we can calculate $\theta_c = \theta_{c'} = arctan(\sqrt{2}tan\theta_3) = 90°$, $66.2°$, $49.9°$, and $29.7°$, respectively.

Experimental setup — The first step of the experiment is to generate polarization-entangled three-qubit GHZ states. Following our previously work [16], as shown in FIG.1, a mode-locked Ti:sapphire laser outputs an infrared(IR) pulse with the central wavelength of 780nm, a pulse duration of 100fs and a repetition of 80MHz, which passes through a LiB_3O_5 (LBO) crystal and is convert to an ultraviolet (UV) light pulse with central wavelength at 390nm. Then the UV light pulse passes through five dichroic mirrors (DM) which are used to separate the mixed infrared and ultraviolet light components. Behind the five DMs, the UV light is focused on a β-barium borate (BBO) crystal to produce a pair of entangled photons $(|H_2H_3\rangle + |V_2V_3\rangle)/\sqrt{2}$ in path 2-3, while the transmitted IR light is attenuated to a weak pseudo single photon source which is prepared in the state $(|H_1\rangle + |V_1\rangle)/\sqrt{2}$ in path 1, where H and V represent horizontal and vertical polarization separately. Then, Photon 2 is combined with photon 1 on a polarizing beam splitter (PBS_{12}). By finely adjusting

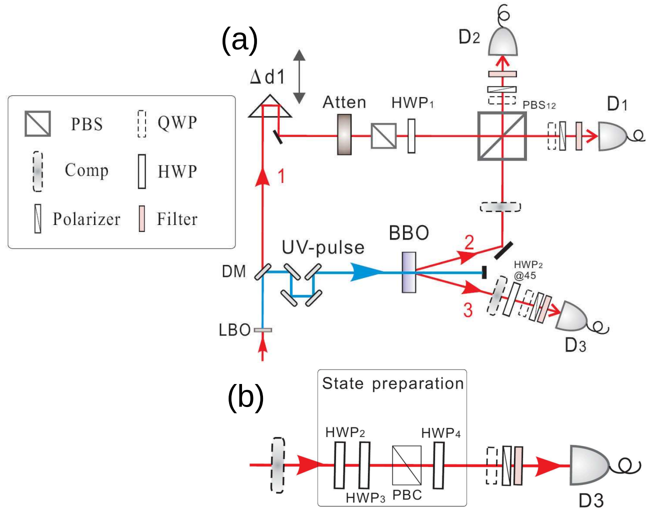

FIG. 1: (Color online) Scheme of the experimental setup. (a) The setup to generate the required three-photon GGHZ state, here setting HWP_2 at 45º. The entangled photons are generated by pumping the UV laser beam on a BBO crystal and a pseudo-single photon source is prepared by attenuating the infrared light after the DM. The average power in the experiment is 90mW and the average two-fold coincidence is $6 \times 10^3 s^{-1}$ in modes 2-3. Prisms $\Delta D1$ is used to ensure that the input photons arrive at the PBS_{12} at the same time. Half-wave plate (HWP) 1 is used to prepare the single photon state $\frac{1}{\sqrt{2}}(|H\rangle_1 + |V\rangle_1)$ and HWP_2 is used to prepare the desired two-photon state. To achieve good temporal and spatial overlap at PBS_{12}, every output is spectrally filtered ($\Delta_{FWHM} = 3nm$) and monitored by fibre coupled single-photon detectors. Throughout the experiment, the coincidence time-window is set to be 5 ns, which ensures that accidental coincidence is negligible. (b) Setup for preparing the MS state. HWP_1 is set at $\pi/8$, and the superposed three-qubit states is GHZ states $\frac{1}{\sqrt{2}}(|H_1H_2H_3\rangle + |V_1V_2V_3\rangle)$. Then we set HWP_3 at 22.5° and can makes the change $|H_3\rangle \rightarrow |+_3\rangle$, $|V_3\rangle \rightarrow |-_3\rangle$. This will convert the GHZ state into $\frac{1}{\sqrt{2}}(|H_1H_2+_3\rangle + |V_1V_2-_3\rangle)$. After that we use a polarization dependent beam splitter cubes (PBC). Therefor the state is $\frac{1}{\sqrt{2}}(|H_1H_2\rangle(a|H_3\rangle + b|V_3\rangle) + |V_1V_2\rangle(a|H_3\rangle - b|V_3\rangle)$, then another half-waveplate (HWP_4) setting at an chosen angle according to the transmission a and b is used behind PBC, its function is as: it changes $a|H_3\rangle + b|V_3\rangle \rightarrow |H_3\rangle$, while $a|H_3\rangle - b|V_3\rangle \rightarrow cos\theta_3|H_3\rangle + \sin\theta_3|V_3\rangle$.

the delay between path 1 and 2 to make sure photon 1 and photon 2 arrived at the PBS_{12} simultaneously, the three-qubit GHZ states $|\psi_{GHZ}\rangle = \frac{1}{\sqrt{2}}(|HHH\rangle + |VVV\rangle)$ can be obtained. In order to get a better fidelity of the output states, we lowered the average power of the laser to 90mw, and the two-photon coincidence count rate to $6 \times 10^3 s^{-1}$. The visibility of two-photon entangled state is 97% in H/V basis, and 95% in $+/-$ basis, where $|+\rangle = \frac{1}{\sqrt{2}}(|H\rangle + |V\rangle)$, $|-\rangle = \frac{1}{\sqrt{2}}(|H\rangle - |V\rangle)$. Using maximum-likelihood technique to construct the density matrix of the state and from the estimated density matrix, we calculate the fidelity characterizing the quality of the state as $F = \langle\psi_{GHZ}|\rho|\psi_{GHZ}\rangle = 0.84 \pm 0.01$.

Next, we generate the GGHZ states and MS states based on the setup we get GHZ states. In order to obtain the GGHZ state $|\psi_g\rangle$, we used a Half-wave plate (HWP_1) (see FIG.1), which is placed behind PBS_1 and set at an angle θ_1. The photon 1 after HWP_1 is prepared in the state $(cos\theta_1 \left|H\right\rangle + sin\theta_1 \left|V\right\rangle)/\sqrt{2}$. By superposing photon 1 with photon 2 on PBS_2, we can get a three-qubit state

$$\left|\psi\right\rangle_{GGHZ} = cos\theta_1 \left|V_1 V_2 V_3\right\rangle + sin\theta_1 \left|H_1 H_2 H_3\right\rangle. \tag{6}$$

For instance, by choosing the $\theta_1 = \pi/4$, the output states will be $\frac{1}{\sqrt{2}}(\left|HHH\right\rangle + \left|VVV\right\rangle)$, which is exactly GHZ states. From the experimental results, we calculate θ_1 by following the equality

$$\theta_1 = \arcsin\sqrt{N_{HHH}/(N_{HHH} + N_{VVV})} \tag{7}$$

where N_{HHH} and N_{VVV} denote three-fold coincidence counts in the basis $H_1H_2H_3$ and $V_1V_2V_3$. In the experiment, we have measured the fidelity and Svetlichny inequality at nine points, which have the proportion of N_{HHH}/N_{VVV} as 1:1, 1:2, 1:4, 1:6, 1:8, 1:10, 1:14, 1:20, 1:60. This will correspond to $\theta_1 = 45^o$, 35.3^o, 26.6^o, 22.2^o, 19.5^o, 17.5^o, 15^o, 12.6^o, and 7.4^o, respectively.

Compared to the generation of the GGHZ states, it is more complicated to generate the MS state $\left|\psi_s\right\rangle$. We carry out the following steps to produce this state. Firstly, HWP_1 is set at $\pi/8$, which will result a three-qubit GHZ state $\frac{1}{\sqrt{2}}(\left|H_1H_2H_3\right\rangle + \left|V_1V_2V_3\right\rangle)$. Secondly, we insert another half-wave plate HWP_3 in path 3, which is set at 22.5° and can makes the change $\left|H_3\right\rangle \rightarrow \left|+_3\right\rangle$, $\left|V_3\right\rangle \rightarrow \left|-_3\right\rangle$. This will convert the GHZ state into $\frac{1}{\sqrt{2}}(\left|H_1H_2 +_3\right\rangle + \left|V_1V_2 -_3\right\rangle)$. Then, we use a polarization dependent beam splitter cube (PBC), which has the properties as: it transmits the horizontal polarization photons with the probability a^2, while for the vertical polarization, the transmission is b^2. The PBC is a custom-made component. The values of a and b can be adjusted through the changing of the axis of PBC. After the PBC, the state becomes $\frac{1}{\sqrt{2}}(\left|H_1H_2\right\rangle(a\left|H_3\right\rangle + b\left|V_3\right\rangle) + \left|V_1V_2\right\rangle(a\left|H_3\right\rangle - b\left|V_3\right\rangle))$. Finally, another half-wave plate (HWP_4) is placed behind PBC and is set at a chosen angle according to the transmission a and b. It has the function as: $a\left|H_3\right\rangle + b\left|V_3\right\rangle \rightarrow \left|H_3\right\rangle$, and $a\left|H_3\right\rangle - b\left|V_3\right\rangle \rightarrow cos\theta_3\left|H_3\right\rangle + \sin\theta_3\left|V_3\right\rangle$, where $\theta_3 = arcsin[b/(a+b)]^{1/2}$. All these steps will result a MS state as

$$\left|\psi_s\right\rangle = \frac{1}{\sqrt{2}}\{\left|H_1H_2H_3\right\rangle + \left|V_1V_2\right\rangle(cos\theta_3\left|H_3\right\rangle + sin\theta_3\left|V_3\right\rangle)\}. \tag{8}$$

Experimental result — In order to characterize the prepared three-qubit GGHZ states and MS states for different θ_1 and θ_3, we have extracted their density matrices by the method of over-complete state tomography [17]. This is implemented by collecting the experimental data for 20s for each of 216 combinations of measurement basis $\{\left|H\right\rangle, \left|V\right\rangle, \left|+\right\rangle, \left|-\right\rangle, \left|R\right\rangle, \left|L\right\rangle\}$, where $\left|R\right\rangle = \frac{1}{\sqrt{2}}(\left|H\right\rangle + i\left|V\right\rangle)$ and $\left|L\right\rangle = \frac{1}{\sqrt{2}}(\left|H\right\rangle - i\left|V\right\rangle)$. With these data, maximum-likelihood technique is used to construct the density matrix of the state. The results are shown in FIG. 2, from which we can see that the fidelities of GGHZ states and MS states for different θ_1 and θ_3 are all lager than 0.8.

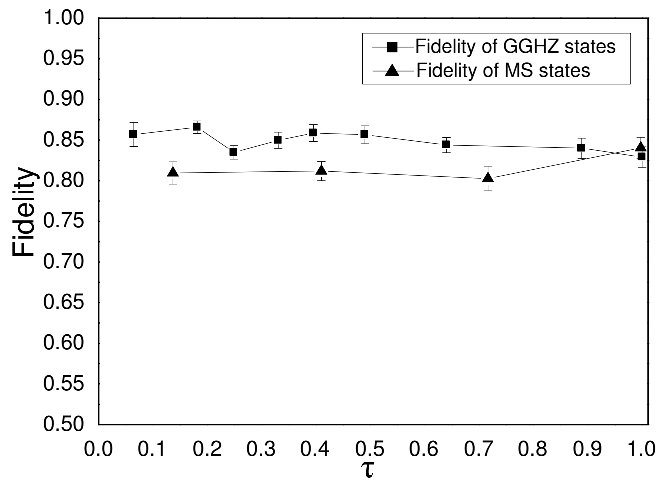

FIG. 2: Fidelity of GGHZ states and MS states. The $fidelity = \left\langle\psi\right|\rho\left|\psi\right\rangle$. Each experimental value is obtained by measuring in an average time of 120 seconds. The error bar of the fidelity is calculated by performing a 100 run Monte Carlo simulation of the whole state tomography analysis, with Poissonian noise added to each experimental data in each run.

Based on the generated state in Eq.(8) and (10) and the special choosed angles in Eq.(6) and (7), we have measured the Svetlichny inequality. The concrete results are given in FIG. 3. For each measurement point, we have collected the data for 120s. In FIG. 3, we have plotted the experimental Svetlichny operator values and the one calculated from the estimated state density matrices. The theoretical values are also drawn using dashed line in FIG. 3. From the experimental results, we can draw three conclusions: first, the experimental violation of Svetlichny inequality is well consist with the one predicted by quantum mechanics given the reconstructed density matrix; second, for the MS states, the amount of violation increases linearly following the increase of the degree of tripartite entanglement, while for GGHZ states there is a minimal value of the violation when the degree of tripartite entanglement is 1/3. Third, the experimental values of the violation are smaller than the theoretical values. There are two important reasons for the experimental non-ideal data. On the one hand, the multi-pair generation of entangled states contributes the main noise of the results due to the probabilistic character of parametric down conversion sources. On the other hand, the imperfection of the linear optics elements such as beam splitter also makes the results non-ideal.

Conclusion — In summary, in our experiment, the series of GGHZ states and MS states with high fidelity $F > 0.8$ have been prepared and we have demonstrated the test of Svetlichny inequality with these states. Tripartite entanglement versus tripartite nonlocality in three-qubit GHZ-class states has been experimentally reported.

There are many open experimental and theoretical questions which are worthy to investigate in the future. Theoretically, it is interesting to generalize the relationship of entanglement and nonlocality into the case of entangled states

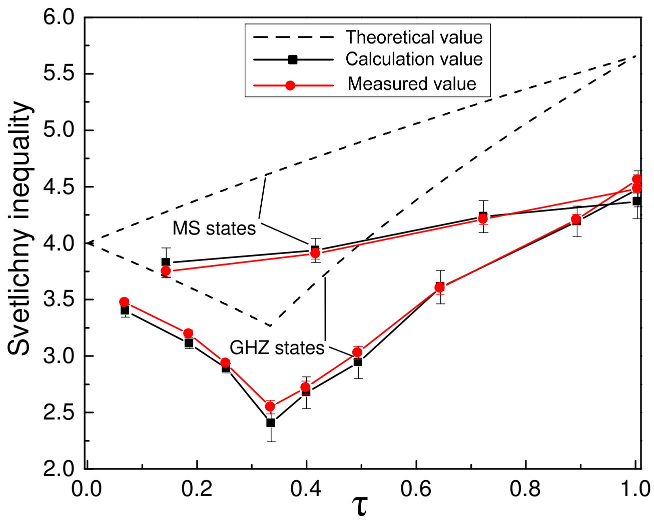

FIG. 3: (Color online) Experimental results. The dashed line show the plot of Eq. (3) and (4) for $S_{max}(\psi_g)$ versus τ for the GGHZ states[9]. The labelled line show the experimental result of Svetlichny inequalities. Where calculation value is calculated from the state density matrix and measured value is measure value of Svetlichny operator.

with more than three qubits. Also, it is worthy to study the Svetlichny inequality for other type of state, such as W state [18]. Third, since there is a certain relationship of the multipartite entanglement and nonlocality, we could use certain Bell inequalities to detect the genuine multi-party entanglement. For a specific state, how to obtain the optimum witness is an important research direction. Finally, there are various types of Bell inequalities for three-qubit generalized GHZ state, such as MABK inequality [19–21], Gisin inequality [22], Zukowski-Brukner inequality [23, 24] and Svetlichny inequality [25]. In the future, it should be interesting to investigate which one is more robust against the noise, and thus more suitable to characterize states.

We thank Wei-Bo Gao for valuable discussions. This work was supported by the Natural Science Foundation of China (Grant No. 60878001) and by the Natural Science Foundation of Shandong Province (Grant No.Y2006A24) and by the Science and Technology Development Program of Shandong Province(Grant No.2010GGX10118).

[1] W. Tittel, H. Zbinden and N. Gisin, *Phys. Rev. Lett.* **81**, 3563(1998).
[2] N. Gisin, *Science.* **326**, 1357(2009).
[3] D. N. Matsukevich, P. Maunz, D. L. Moehring, S. Olmschenk and C. Monroe, *Phys. Rev. Lett.* **100**, 150404(2008).
[4] J. L. Chen, D. L. Deng, *Phys. Rev. A* **79**, 012115(2009).
[5] P. R. Tapster, J. G. Rarity and P. C. M. Owens *Phys. Rev. Lett.* **73**, 1923(1994).
[6] J. F. Clauser, M. A. Horne, A. Shimony and R. A. Holt, *Phys. Rev.Lett.* **23**, 880(1969).
[7] N. Gisin, *Phys. Lett. A* **154**, 201(1991).
[8] S. Popescu and D. Rohrlich, *Phys. Lett. A* **166**, 293(1992).
[9] S. Ghose, N. Sinclair, S. Debnath, P, Rungta and R. Stock, *Phys. Rev. Lett.* **102**, 250404(2009).
[10] H. A. Carteret and A. Sudbery, *J. Phys. A.* **33**, 4981(2000).
[11] J. C. Howell, A. L. Linares and D. Bouwmeester, *Phys. Rev. Lett.* **88**,030401(2002).
[12] K. Mattle, H. Weinfurter, P. G. Kwiat and A. Zeilinger, *Phys. Rev. Lett.* **76**, 4656(1996).
[13] J. Lavoie, R. Kaltenbaek and K. J. Resch, *New J. Phys.* **11**, 073051(2009).
[14] V. Coffman, J. Kundu and W. K. Wootters, *Phys. Rev. A* **61**, 052306(2000).
[15] C. Emary and C. W. J. Beenakker, *Phys. Rev. A* **69**, 032317(2004).
[16] H. X. Lu, J. Zhang, X. Q. Wang, Y. D. Li and C. Y. Wang, *Phys. Rev. A* **78**, 033819(2008).
[17] K. J. Resch, P. Walther, and A. Zeilinger, *Phys. Rev. Lett.* **94**, 070402(2005).
[18] W. Dur, G. Vidal, and J. I. Cirac, *Phys. Rev. A* **61**, 062314(2000).
[19] N. D. Mermin, *Phys. Rev. Lett.* **65**, 1838(1990).
[20] M. Ardehali, *Phys. Rev. A* **46**, 5375(1992).
[21] A. V. Belinskii and D. N. Klyshko, *Phys. Usp.* **36**, 653(1993).
[22] J. L. Chen, C. Wu, L. C. Kwek and C.H. Oh, *Phys. Rev. A* **78**, 032107(2008).
[23] M. Zukowski, C. Brukner, W. Laskowski and M. Wiesniak,, *Phys. Rev. Lett.* **88**, 210402(2002).
[24] M. Zukowski and C. Brukner, *Phys.Rev. Lett.* **88**, 210401(2002).
[25] G. Svetlichny, *Phys. Rev. D* **35**, 3066(1987).